

# GEOPHYSICS

## Array estimators and the use of microseisms for reconnaissance of sedimentary basins

M. W. Asten\* and J. D. Henstridge†

### ABSTRACT

A "natural field" seismic technique is possible to attain by observing microseisms with a suitably designed array and by digitally processing the data to obtain estimates of the phase velocities of Rayleigh waves. Wavelengths of interest in detecting depth to the basement of sedimentary basins are in the range 2 to 20 km, and correspond to wave periods from 1 to 7 s. An array of five or seven seismometers deployed as an expanding cross configuration simplifies field procedures and is adequate for phase velocity measurements of Rayleigh waves in the required wavelength range, provided high-resolution frequency-wavenumber spectral analysis is used. This analysis can be implemented on a minicomputer in the field.

Results obtained from observation in a sedimentary basin of known structure show predominantly fundamental-mode Rayleigh wave propagation. The scatter of velocity estimates is small enough to allow inversion by curve matching, and depth to the basement can be computed to an accuracy of  $\pm 30$  percent without requiring restrictive assumptions of a seismic velocity structure.

### INTRODUCTION

The high cost of regional on-shore seismic surveys using conventional reflection or refraction methods poses the question of whether passive or natural field seismic methods may be cost-effective for regional reconnaissance surveys. In this paper, we discuss the effectiveness of one such technique, and note that the cost in terms of instrumentation and logistics

appears favorable for acquisition of low-resolution seismic data. Naturally occurring seismic waves, termed microseisms or seismic noise, can be detected over a period range of at least 0.01 to 100 s. However, since the wave motion is in general restricted neither to a single mode nor to a single direction of propagation, extraction of useful information requires use of an array of geophones combined with digital data processing techniques.

The method described in the paper utilizes the fact that microseisms in the period range 2 to 20 s propagate principally as Rayleigh waves, and exhibit phase velocity dispersion which is a function of the velocity structure of the upper few kilometers of the Earth's crust. An elementary discussion of Rayleigh waves in sedimentary rock overlying crystalline basement was given by Tatham (1975). More rigorous discussions were given by Dorman and Prentiss (1960), McEvilly and Stauder (1965), and Mooney and Bolt (1966).

Toksöz (1964) reported an earlier attempt to use microseisms in the exploration of sedimentary basins. The advances in array data processing theory and available computers since that experiment make a further study of the method worthwhile. In this study, two major tasks are recognized: (1) the design of a seismic array which is logistically viable in a reconnaissance exploration program; and (2) the implementation of optimum data processing procedures on a minicomputer in the field.

### SOURCES AND PROPAGATION MODES OF MICROSEISMS

Generating sources and propagation modes of microseisms were reviewed by Asten (1976) and are summarized in Figure 1. Wave action at coast lines appears to be the most important source of microseisms at periods within the 2 to 18 s band. Although such microseisms have been studied by seismologists for decades, it was only with the advent of seismic arrays such

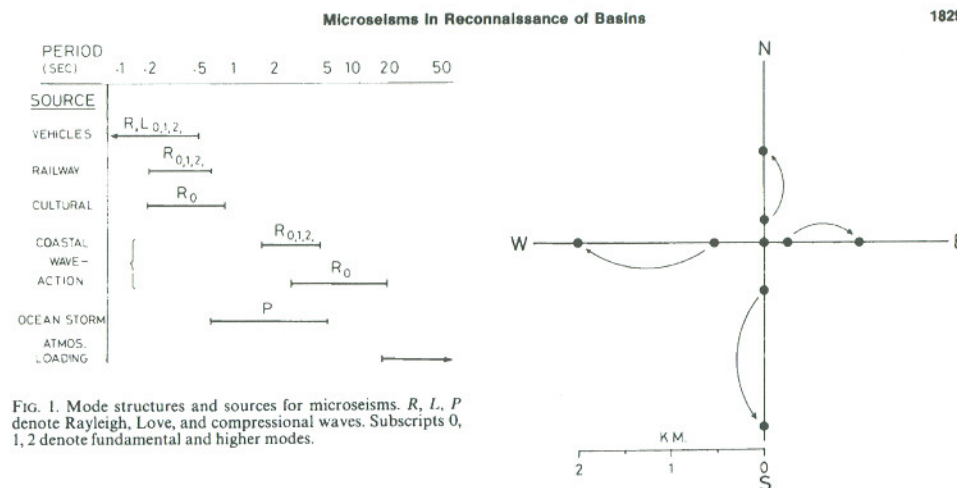


FIG. 1. Mode structures and sources for microseisms.  $R$ ,  $L$ ,  $P$  denote Rayleigh, Love, and compressional waves. Subscripts 0, 1, 2 denote fundamental and higher modes.

as the Montana Large Aperture Seismic Array (LASA) that microseism sources and propagation modes were resolved in any detail (Haubrich and McCamy, 1969; Toksöz and Lacoss, 1968). For periods 6 to 20 s, propagation occurs as fundamental and higher mode surface waves. At periods 2 to 6 s, both surface and  $P$ -wave propagation modes have been recorded at the LASA, with a proportion of  $P$ -wave microseism energy being dependent upon the presence of ocean storms near the continent. Phase velocity measurements by Toksöz (1964) in three sedimentary basins of North America yielded values consistent with fundamental Rayleigh mode propagation in the period range 1.3 to 6 s.

From the above information, we may conclude that the Rayleigh modes necessary for this technique of sedimentary basin reconnaissance exist, but the distribution of energy between Rayleigh modes, and the proportion of accompanying  $P$ -wave "noise" is dependent upon both locality and meteorologic factors.

An interesting consequence of the source and propagation mode of surface waves is that they are only minimally affected by thin, irregular top layers (e.g., basalt cover) which present significant problems to conventional seismic techniques.

### DESIGN OF AN ARRAY

For the ideal case of a single noise-free plane wave propagating in a single direction, the vector phase velocity is readily computed from the relative phases of the signal recorded at three geophones in a triangular array. In fact, such an array could be used even if noise were present, but only if the noise structure were accurately known (for example, the noise at each geophone not correlated with the noise at the other geophones), and if the signal could be observed for an indefinitely long time to allow the effects of noise to average out. However, in practice, noise will be present, and it will only be possible to observe for a limited time, since the microseismic signals have finite duration and there may be more than one plane wave present.

FIG. 2. The expanding seismic array: five geophones are used to form arrays of diameter 0.75, 1.5, and 3 km. Only two geophones are moved for each expansion.

The limitations of such an array can only be overcome by using more geophones to introduce "redundancy of information" and beamforming data processing methods to make best use of the information collected. In this paper we consider use of "conventional" and "high-resolution" wavenumber spectra as developed by Lacoss et al. (1969), Capon (1969), and reviewed by Davies (1973), Capon (1973), and Filson (1975).

Four constraints apply in designing the array configuration.

- (1) The array diameter ( $D$ ) should be at least as large as the longest wavelength of interest to give adequate resolution of long wavelengths. This condition ensures that the array function will have a null point. For a Rayleigh wave of period 6 s and velocity of 3 km/s, this implies that  $D \geq 18$  km.
- (2) When viewed from any direction, there must be some stations whose spacings are less than half the shortest wavelength of interest so as to avoid aliasing in the wavenumber domain. For Rayleigh waves of a 1 s period this may require a spacing less than 0.75 km.
- (3) The number of stations must be greater than the number of plane waves which may be present at any one time. This is particularly a problem with microseismic work.
- (4) The deploying of the array must remain logistically viable in the context of a reconnaissance exploration program. If a single array is used, the conflicting constraints of (1) and (2) require the use of a large number of seismometers with cable or telemetry links to a central recording site. Instead an asymmetrical cross configuration has been designed (Asten 1976).

Presented in part at the 47th Annual International SEG Meeting, Calgary, 1977. Manuscript received by the Editor January 30, 1980. Revised manuscript received April 20, 1984.

\*Formerly Macquarie University, N.S.W., Australia; presently Broken Hill Proprietary Co. Ltd., P. O. Box 559, Camberwell, Vic. 3124, Australia.

†Biometrics Unit, University of Western Australia, Nedlands, W.A. 6009, Australia.

© 1984 Society of Exploration Geophysicists. All rights reserved.

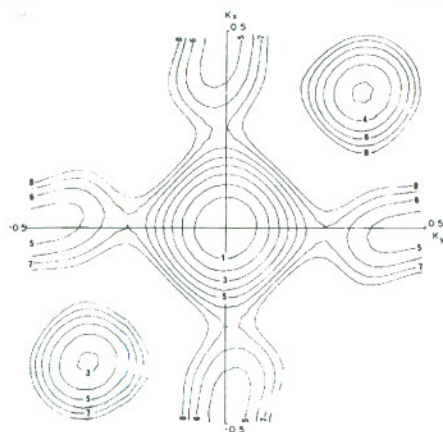


FIG. 3. Conventional array response of a five-geophone 3 km diameter array.

1977a) which can be expanded progressively by moving only two stations at a time while keeping the same basic geometry as shown in Figure 2. The expansion is repeated with microseism data recorded at each stage until the range of array diameters used covers the range of wavelengths of interest.

#### TECHNIQUES OF WAVENUMBER ANALYSIS

Conventional frequency-wavenumber spectral analysis is the simplest technique for extraction of propagation velocities of the different frequency components in a recorded microseism, both from the conceptual and the computational viewpoints. In fact, in the nondispersive situation, it is identical to delay-and-sum beamforming. With this method, one may either consider the full frequency range at once using a model for the dispersion as a function of frequency (see e.g., Goncz and Hannan, 1975) or consider the frequency bands one at a time. We follow the latter approach since it requires fewer assumptions about the data.

The estimate of the scaled power spectral density at angular frequency  $\omega$  and vector wavenumber  $\mathbf{k}$  for an array of  $p$  geophones is

$$\hat{P}(\omega, \mathbf{k}) = \sum_{j=1}^p \sum_{l=1}^p \hat{c}_{jl}(\omega) \exp(-i2\pi\mathbf{k} \cdot \mathbf{r}_{jl}),$$

where

$\hat{c}_{jl}(\omega)$  = an estimate of the complex coherency between signals at the  $j$ th and  $l$ th geophones at frequency  $\omega$ ,

$\mathbf{r}_{jl} = \mathbf{r}_j - \mathbf{r}_l$  where  $\mathbf{r}_j$  and  $\mathbf{r}_l$  are the positions of the  $j$ th and  $l$ th geophones,

$$|2\pi\mathbf{k}| = \omega/|\mathbf{v}|,$$

and

$\mathbf{v}$  = phase velocity of wave motion at frequency  $\omega$ .

Note that wavenumber is defined to have a direction *anti-parallel* to the direction of propagation with units of cycles/kilometer.

This expression can be conveniently written in matrix form as

$$\hat{P}(\omega, \mathbf{k}) = \mathbf{E}(\mathbf{k})^* \mathbf{C}(\omega) \mathbf{E}(\mathbf{k})$$

where

$$\mathbf{E}(\mathbf{k}) = (e^{-i2\pi\mathbf{k} \cdot \mathbf{r}_1}, \dots, e^{-i2\pi\mathbf{k} \cdot \mathbf{r}_p})^T,$$

and  $\mathbf{C}(\omega)$  is the matrix of coherencies. Superscripts  $*$  and  $T$  refer to conjugate transpose and normal transpose, respectively. We shall call  $\mathbf{E}(\mathbf{k})$  the phase vector.

A single monochromatic plane wave of frequency  $\omega$  and wavenumber  $\mathbf{k}_0$  differs only in phase at each station. Therefore it has a coherency-distance relation of the form

$$c(\omega, \mathbf{r}) = \delta(\omega - \omega_0) \exp(i\mathbf{k}_0 \cdot \mathbf{r}),$$

and [as shown by Capon (1969, 1970)] has a frequency-wavenumber spectrum of the form

$$P(\omega, \mathbf{k}) = \delta(\omega - \omega_0, \mathbf{k} - \mathbf{k}_0),$$

which is a delta function in three-dimensional space. When finite lengths of data are acquired with a finite array, the estimated power spectrum for such a monochromatic wave is

$$\hat{P}(\omega, \mathbf{k}) = |W_t(\omega - \omega_0)|^2 |W_s(\mathbf{k} - \mathbf{k}_0)|^2$$

where  $W_t(\omega)$  is the Fourier transform of the time window used for the data recorded from each geophone, and

$$|W_s(\mathbf{k})|^2 = \sum_{j=1}^p \sum_{l=1}^p \exp(-i2\pi\mathbf{k} \cdot \mathbf{r}_{jl}).$$

$|W_s(\mathbf{k})|^2$  is termed the spatial window function (Lacoss et al., 1969) or the beamforming array response (Capon, 1969). For the more general case of true spectrum distributed in wavenumber magnitude and azimuth, it may be shown that the estimated wavenumber spectrum is the 2-D convolution of the true spectrum with the spatial window function (Lacoss et al. 1969, p. 25).

The array response of the five-station cross array with arm-lengths 1 km and 2 km, is shown in Figure 3. The response power is shown in decibels down with respect to maximum, contoured on wavenumber space.

If only one plane-wave signal, with wavenumber  $\mathbf{k}_0$ , propagates in the presence of incoherent noise, then the only purpose of using  $\hat{P}(\omega, \mathbf{k})$  is to obtain an estimate of  $\mathbf{k}_0$ . Any other features of the estimate of the wavenumber spectrum will be artifacts of the spatial window function of the array. We can use the fact that  $W_s(\mathbf{k})$  will always have a global maximum when  $\mathbf{k} = 0$ , and hence  $\hat{P}(\omega, \mathbf{k})$  will have a maximum when  $\mathbf{k} = \mathbf{k}_0$ . This was discussed by Hannan (1975) who gave a general statistical treatment of the errors of estimation, including error variances as a function of the true spectra and the array design. In fact it can easily be shown that his methods provide an estimate which is very close to the true optimal maximum likelihood estimator of  $\mathbf{k}_0$ .

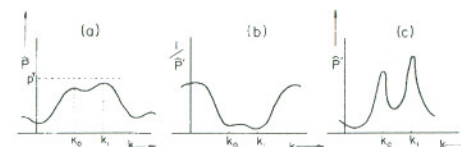


FIG. 4. Illustrative comparison of the conventional and HR wavenumber estimators on data containing two wavenumbers  $\mathbf{k}_0$  and  $\mathbf{k}_1$ . (a) Conventional estimator  $P$  yields poorly resolved maxima. (b) Summation using the inverse of the coherency matrix yield near-zero minima instead of maxima at  $\mathbf{k}_0, \mathbf{k}_1$ . (c) Inverse of (b) is  $P'$ , showing sharp maxima at  $\mathbf{k}_0, \mathbf{k}_1$ .

If the noise is not incoherent, this simple method of estimating  $\mathbf{k}$  is not unbiased, and in fact unless the noise has particular structure or the signal-to-noise ratio is very high, estimates of  $\mathbf{k}$  can be very poor. Even an isotropic noise field (Eckart, 1953) can bias results. If, however, the structure of the noise field is known (in terms of the correlations between geophones), Henstridge (1977) showed it is possible to allow for it and obtain useful estimates equivalent to those of Hannan (1975).

#### Resolution

Unfortunately, in seismic problems the coherent noise is usually another signal or signals with unknown spectral structure; hence it is more useful to consider methods which aim at estimating the wavenumbers  $\mathbf{k}_1, \mathbf{k}_2, \dots, \mathbf{k}_s$  of all the signals present ( $s$  represents the number of signals). Hence the resolution of the array becomes important. The Rayleigh criterion used in optics would consider two signals with wavenumbers  $\mathbf{k}_1$  and  $\mathbf{k}_2$  resolved if the difference  $|\Delta\mathbf{k}|$  is greater than the radius of the first null or zero point of the array response function. This is often considered too conservative, and Woods and Lintz (1973) proposed a criterion whereby  $|\Delta\mathbf{k}|$  must exceed the radius of the 3 dB contour of the array response function. These radii are dependent upon the array diameter and, to a lesser extent, on array geometry. The criterion for resolution may thus be written as

$$|\Delta\mathbf{k}| \geq r/D$$

and resolving power RP defined by

$$RP = r^{-1}$$

where  $D$  is the array diameter and  $r$  is a constant determined by array geometry. For practical circular and cross arrays (using conventional beamforming methods), RP takes values in the range 5 to 7 by Rayleigh's criterion or 1.8 to 2.5 by Woods and Lintz's (1973) criterion.

With arrays of the type discussed in this paper the diameter is comparable with or less than the wavelengths of interest, and so the conventional wavenumber estimate suffers from very poor resolution. Capon (1969) introduced a new high-resolution (HR) estimate of power spectral density given by

$$\hat{P}(\omega, \mathbf{k}) = [\mathbf{E}(\mathbf{k})^* \mathbf{C}(\omega)^{-1} \mathbf{E}(\mathbf{k})]^{-1} \quad (2a)$$

or

$$\hat{P}(\omega, \mathbf{k}) = \left\{ \sum_{j=1}^p \sum_{l=1}^p \hat{c}_{jl}(\omega) \exp[-i2\pi\mathbf{k} \cdot \mathbf{r}_{jl}] \right\}^{-1}, \quad (2b)$$

where the  $\hat{c}_{jl}(\omega)$  are the elements of  $\mathbf{C}(\omega)^{-1}$ . This estimate of  $\hat{P}(\omega, \mathbf{k})$  was based on principles of maximum likelihood filtering, and other justifications have followed (Capon, 1973; Liaw, 1977). These results state that  $\hat{P}(\omega, \mathbf{k})$  can be a good estimate of the true wavenumber spectrum  $P(\omega, \mathbf{k})$ , not necessarily that  $\hat{P}(\omega, \mathbf{k})$  can be used to estimate the wavenumber of a signal.

Figure 4 shows a simple graphical explanation of the HR estimator. The explanation is illustrative, not exact, since the HR estimator is capable of resolving two wavenumbers which remain entirely unresolved by the conventional estimator.

In comparing properties of the two estimators, we distinguish between their accuracy and their resolution. In Appen-

dix A it is shown that when only one signal is present the maxima of  $\hat{P}(\omega, \mathbf{k})$  and  $\hat{P}'(\omega, \mathbf{k})$  coincide; hence they are equally accurate in estimating the wavenumber of that signal. This is consistent with the proof by Pisarenko (1972) that both the conventional estimate and Capon's estimate belong to a general class of estimates which share many properties.

In a study of microseisms one cannot rely upon there being only one signal. There will often be several signals and these may have some common origins. For example, two signals may originate from the same source but have different modes of propagation and hence different velocities. Woods and Lintz (1973) considered the case of two correlated signals  $\mathbf{k}_0$  and  $\mathbf{k}_1$ , plus noise which was uncorrelated between stations but of arbitrarily low level. They showed, theoretically, that  $\hat{P}(\omega, \mathbf{k})$  will be zero except when  $\mathbf{k} = \mathbf{k}_0$  or  $\mathbf{k}_1$ , and hence resolving power is arbitrarily high for arbitrarily low noise levels. In Appendix B this is extended to the case of an arbitrary number of signals in uncorrelated noise, a situation more realistic in studies of microseisms.

Unfortunately, it is difficult to predict quantitatively the improvement in resolution obtainable by using the HR estimator on real data. Empirical results by Woods and Lintz (1973) and Asten (1976) show the HR estimator to have a resolving power three to six times greater than the conventional estimator. However the widths of peaks are very dependent upon signal-to-noise ratio as well as signal properties and array design, so the improvement cannot be regarded as a general characteristic of the estimator.

#### Bias

Both the conventional and HR estimators in general produce biased estimates when multiple wavenumbers are present. One source of bias to high velocities is attributable to the finite-size grid in wavenumber space (Bungum and Capon, 1974). This bias is predictable, quantifiable, and reducible by the use of smaller grid spacing. A second source of bias is due to the smearing effect of the array response function. Modeling with the conventional estimator (Asten, 1977a) shows bias to be most apparent when two plane waves  $\mathbf{k}_1$  and  $\mathbf{k}_2$  with different azimuths are incompletely resolved in wavenumber space; the wavenumber yielded by the estimator is then approximately a vector mean of the true wavenumbers, and in most cases has a

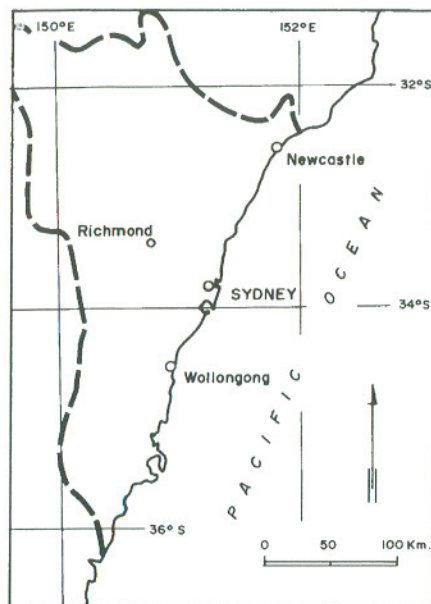


FIG. 5. Location of test site at Richmond, in the Permo-Triassic sedimentary Sydney basin, Eastern Australia. The dashed line shows northern and western limits of the basin (from Mayne et al., 1974).

smaller magnitude (corresponding to a higher propagation velocity) than either  $k_1$  or  $k_2$ . A general condition for avoiding biasing is that the array response function when centered on  $k_1$  should possess a minimum at  $k_2$  (d'Assumpcao, 1977). Although it may be possible to do this by shaping the array response function with suitably weighted coherencies, the data-adaptive approach needed appears unsuited to the handling of large amounts of seismic data.

The HR estimator reduces biasing by resolving multiple wavenumbers. However, an additional condition for successful application of the method is that the coherency matrix elements  $\hat{c}_{ij}$  in equation (2) be nonsingular and hence possess a stable inverse. Capon (1969) showed that a necessary but not sufficient condition for nonsingularity is that

$$M \geq p, \quad (3)$$

where  $M$  = number of discrete frequencies averaged for each coherency estimate. The condition becomes insufficient if unsmoothed spectral values within the frequency window are partially correlated; this will occur if the signals analyzed contain transients (Capon, 1969) or if the time window applied before transformation is not square (Henstridge, 1977). The practical effect of using a near-singular matrix is to give HR

Table 1. Seismic model for Sydney basin near Richmond.

Thickness (m)	$P$ (km/s)	$S$ (km/s)	$v$	$\rho$ ( $t/m^3$ )
1.5	0.3	0.15	0.33	1.8
18.3	0.71	0.39	0.28	2.0
8.5	1.7	0.39	0.47	2.2
(Alluvium base)				
500	3.48	1.88	0.30	2.4
1 000	3.88	3.23	0.25	2.5
1 800	4.63	2.68	0.25	2.6
(Metamorphosed basement)				
4 000	6.04	3.49	0.25	2.8
25 000	6.5	3.75	0.25	2.9
(Moho)				
—	8.0	4.6	0.25	3.3

wavenumber plots which are unstable with respect to changes in data length or frequency window used, and therefore yield unreliable wavenumber estimates (Asten, 1976).

A nonsingular coherency matrix is assured if a small amount of incoherent noise is added to the matrix elements  $\hat{c}_{ij}$  prior to inversion (Capon, 1969). This is most simply accomplished by multiplying the diagonal elements  $\hat{c}_{ii}$  by a factor  $D$  slightly greater than unity. A series of tests described by Asten (1976) showed that with  $D = 1.00$ ,  $M = 10$ , and  $N = 7$ , HR wavenumber plots were stable if a square time window was used, but occasionally were unstable if a Hanning time window was used. With  $D = 1.02$ ,  $M = 10$ , and  $N = 7$ , HR wavenumber plots were stable irrespective of the time window used, and showed no significant loss in resolution. Further increase in the value of  $D$  did not further improve stability, but it did reduce resolution. Thus the value  $D = 1.02$  is preferred for HR plots involved in this study.

#### INSTRUMENTATION AND FIELD PROCEDURES

Seven Willmore Mk II geophones and TAM-5 seismic amplifiers were made available for the project by the Australian Bureau of Mineral Resources. The geophones were not identical, but were calibrated for absolute amplitude and phase response using techniques described by Asten (1977b). Relative phase response of the amplifiers was within 3 degrees over the frequency range of interest.

A test site in the Sydney basin, located near Richmond, 50 km west of Sydney (Australia) was chosen (Figure 5). Table 1 shows a layered seismic model for the site, based on compressional-wave data from a local seismic refraction survey and from oil company seismic reflection surveys, plus assumed Poisson ratios and densities for consolidated rock. Poisson ratios for the alluvium were obtained from a separate experiment (Asten, 1978b).

The array configuration of Figure 2 was adhered to as far as possible, within constraints imposed by access and available instrumentation. The smallest cross array used contained seven vertical-component geophones and had an aperture of 750 m. Seismic amplifiers were located within 5 m of each geophone,

and the amplified signal was connected to a minicomputer by twin wires laid from a vehicle. The computer was a Interdata 70 equipped with A/D and D/A converters and a nine-track tape drive, all mounted in a caravan.

Manpower for the survey consisted of one geophysicist plus one assistant with a light vehicle.

Two expansions of the array, to 1.5 km and 3 km diameter, were executed, with the number of stations reduced from seven to five for logistical reasons. In order to reduce the connecting wire needed for these larger diameters, signals from two stations were transmitted to the computer via simple radio-telemetry links constructed from standard audiofrequency modems and pairs of high-frequency band transceivers (Asten, 1976).

Microseism data were acquired in segments of length 40 or 80 s with a sample interval of 10 or 20 ms, and were stored as files of multiplexed samples on the digital tape.

#### DATA PROCESSING

Each segment (or file) of digital data was processed with the following steps.

(1) Demultiplex. Compute raw spectrum for each station with a Hanning (cosine-bell) time window and a standard fast Fourier transform routine; correct spectrum for the combined transfer function of geophone, amplifier and filters; store true ground-acceleration spectra on digital tape. The Hanning time window, rather than a square window, was required to minimize frequency-window leakage effects from spectral peaks. Such leakage, if not eliminated, results in erroneous phase velocity estimates (Smart, 1971).

(2) Estimate complex coherencies between stations using smoothing over 10 discrete frequencies with square frequency windows; store the array coherency matrix for each frequency window on tape. The theory used in this step follows Koopmans' (1974) approach.

(3) For each coherency matrix, compute HR wavenumber transform on a  $41 \times 41$  point grid in wavenumber space; display power density on the grid as a "density plot" on the computer's printer. (These density plots prove sufficiently accurate for estimating wavenumbers, and thus the need for additional software and hardware to produce contour maps in the field is avoided.)

(4) Pick maxima from wavenumber plots; convert to velocities; plot velocities versus frequency on bilogarithmic graph paper.

#### RESULTS

For each of the three cross arrays used, analog chart records of each file of data were visually scanned to reject data containing anomalous noise, strong high-frequency signals (e.g., from vehicular traffic), or below-average signal strength at periods 2 to 6 s. Four or six files of data for each array were processed to obtain phase velocity estimates from HR wavenumber plots. Figure 6 shows an example of three HR plots produced from three adjacent frequency windows on a single data file.

Phase velocities obtained are shown in Figures 7, 8, and 9.

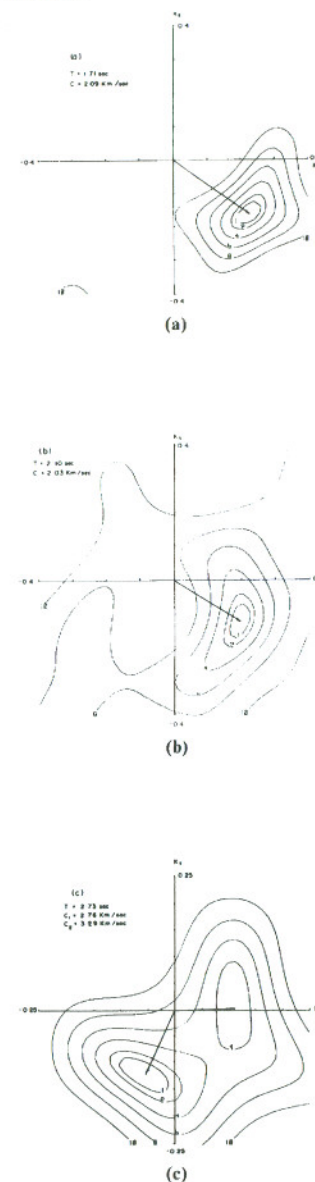


FIG. 6. HR wavenumber plots for three consecutive frequency bands of data file T4 F11, acquired with the 3 km array.

For purposes of comparison, theoretical phase velocity dispersion curves for fundamental, first and second higher Rayleigh wave modes are shown on these figures. The theoretical velocities were computed for the model shown in Table 1 using methods described by Dorman and Prentiss (1960).

Phase velocities in the period range 1.5 to 6 s are of most interest since they are more sensitive to the thickness of sedimentary rock over basement. Velocities obtained with the 3 km array (Figure 8) show clear dispersion consistent with fundamental mode Rayleigh wave propagation. The scatter of velocity estimates is controlled by array resolution. Since the wavelengths being considered range up to 18 km (at 6 s period) compared with an array diameter of 3 km, it is reasonable to suppose that a reduction in scatter of velocity estimates could be achieved by further expanding the array to 6 km and 12 km diameters.

In the period range 0.5 to 1 s, velocity estimates show considerable scatter on Figures 7 and 8 and do not show any trend relating to Rayleigh wave velocities. We may note, however, that power density spectra of ground motion show a strong minimum in this band (e.g., see Figures 9 and 10 of Asten, 1978a), and that previous microseism surveys summarized in Figure 1 have also failed to define a dominant source or mode for microseisms in this band.

At periods shorter than 0.5 s phase velocity estimates obtained with the 0.75 km array (Figure 7) are indicative of fundamental and higher mode Rayleigh wave propagation. These waves are sensitive to seismic properties of the top few hundred meters of sediments, and thus their possible uses lie not in sedimentary basin reconnaissance but in depth-of-alluvium or depth-of-weathering studies. These aspects have been published elsewhere (Asten, 1978b).

#### Resolution of basin depth

The question of greatest interest is to what accuracy do observed phase velocities define sedimentary basin depth. Phase velocity data plotted on bilogarithmic graph paper can be compared with master curves of Rayleigh wave dispersion, by using curve-matching procedures similar to those used as standard procedures in electrical geophysical methods.

An established procedure for reduction of the number of master curves necessary is to use the upper-layer shear velocity ( $\beta_1$ ), thickness ( $h_1$ ), and density ( $\rho_1$ ) as units of velocity, distance, and density. Computed dispersion curves of phase velocity  $C$  versus period  $T$  then take the form of plots of  $C/\beta_1$  versus  $\beta_1 T/h_1$  (see, for example, Dorman, 1959; Mooney and Bolt, 1966). If an observed dispersion curve  $C'$  versus  $T'$  is plotted on bilogarithmic graph paper and overlain on a matching master curve  $C/\beta_1$  versus  $\beta_1 T/h_1$  (where  $\rho_1$  is specified), then

$$\beta_1 = C/C', \quad h_1 = (T/T') \times (C/C'), \quad \text{and} \quad \rho_1$$

are the units of velocity, distance, and density for a corresponding model of this real earth at the field observation sites. In practical terms, the model curve, if plotted on bilogarithmic scales, need not have the dimensionless form.

Thus in an observed dispersion curve  $C'$  versus  $T'$  matches a theoretical curve  $C$  versus  $T$  for an  $n$ -layered seismic model, with axis shifts given by

$$C' = yC,$$

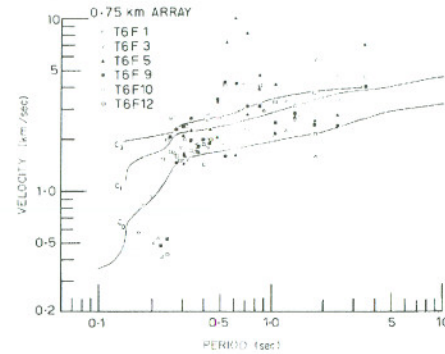


FIG. 7. Velocity estimates in (km/s) made with six files of data from the 0.75 km array using the HR estimator. The superimposed curves are theoretical velocities for fundamental and higher Rayleigh modes.

and

$$T' = xT,$$

where  $x$ ,  $y$  are constants, then seismic parameters (primed symbols) for an  $n$ -layer approximation to the real earth are

$$\beta'_m = y\beta_m \quad (\text{shear velocity}),$$

$$\alpha'_m = y\alpha_m \quad (\text{compressional velocity}),$$

$$h'_m = xyh_m \quad (\text{layer thickness}),$$

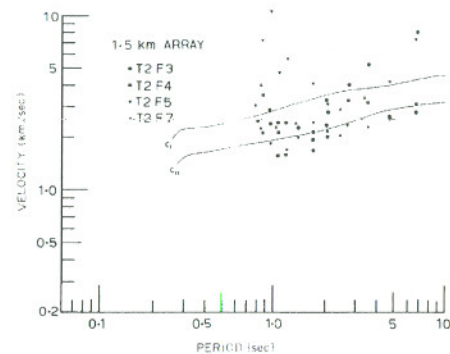


FIG. 8. Velocity estimates made with four files of data from the 1.5 km array.

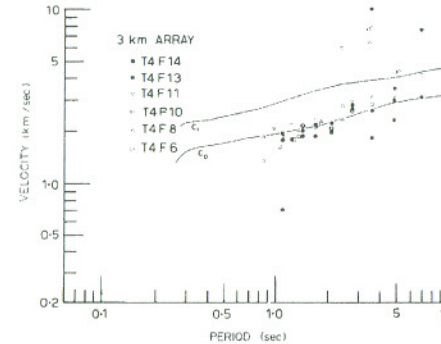


FIG. 9. Velocity estimates made with six files of data from the 3 km array.

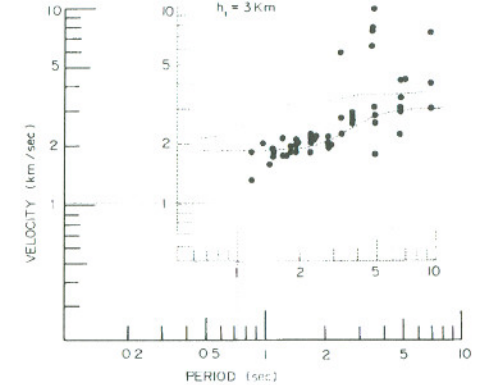


FIG. 10. Data from Figure 9 with superimposed master curves (dashed lines) of Rayleigh wave velocities on a two-layer model representing a sedimentary basin of thickness 3 km.

and

$$\rho'_m/\rho'_1 = \rho_m/\rho_1 \quad (\text{density ratio}),$$

where  $m$  has values 1 to  $n$  for an  $n$ -layer model.

Note that ratios  $\alpha_m/\beta_m$  for each layer must be specified for a given master curve, and remain invariant under the scaling procedure.

In Figure 10 phase velocity observations made with the 3 km diameter array are compared with a theoretical dispersion curve computed for a two-layer model. Parameters of the model are shown in Table 2 and represent a idealized sedimentary basin of depth 3 km, overlying crystalline basement. The fit shown corresponds to  $x = 0.72$  and  $y = 1.06$  in equation (4), thus yielding an estimated basin depth of 2.3 km. Alternative graphical fits of the model curve to the data are equally valid and yield depth estimates in the range 2.2 and 3.7 km, compared with a depth of 3.3 km given in Table 1 which was obtained from geologic mapping and limited seismic reflection data reviewed in Mayne et al. (1974).

In this example the sedimentary basin has been modeled using horizontal layers. Ten kilometers west of the test site the basement rises at a dip of approximately 6 degrees toward a major fault an additional 10 km to the west. For Rayleigh wave periods up to 6 s the fault is a full wavelength or more from the test site. Therefore it is not expected that the lateral geologic variation would induce phase velocity perturbations at the test

Table 2. Seismic model for a "standard" sedimentary basin.

Thickness (m)	$P$ (km/s)	$S$ (km/s)	$v$	$\rho$ ( $t/m^3$ )
3 000	3.5	2.0	.26	2.4
—	6.0	3.5	.25	2.8

site, although it is conceivable that reflected energy may in some circumstances result in additional apparent sources appearing on wavenumber plots.

In a general application of microseism observations to sedimentary basin reconnaissance, assumptions of horizontal layering may not be justified. Interpretation of measured velocities may then require 2-D analog modeling (e.g., Kuo and Thompson, 1963) or finite-element modeling (Drake, 1972).

#### CONCLUSION

Phase velocities of microseisms in the range 0.3 to 7 s have been successfully measured using high-resolution frequency-wavenumber analysis of data from an expanding array of five geophones. Velocity dispersion for periods in the range 2 to 7 s is consistent with fundamental-mode Rayleigh wave propagation, although velocity estimates show some biasing toward higher velocities in accordance with theoretical limitations of the HR estimator. Comparison of velocity data with theoretical Rayleigh wave dispersion curves for two-layer models allows basin depth to be estimated to within 30 percent of geologic depth. It is reasonable to predict that with suitable telemetry equipment, expansion of the seismic array to diameters greater than 3 km would reduce this uncertainty.

Manpower requirements for a survey are low (observer plus 1 or 2 assistants) so the potential exists for gaining low-resolution reconnaissance seismic data at costs below conventional seismic surveys, particularly where irregular surface layers impede the use of conventional seismic techniques.

#### ACKNOWLEDGMENTS

The authors thank Prof. K. Vozoff, Prof. E. J. Hannan, and Dr. D. W. King for their interest and advice. Software for digital data acquisition in the field was written by Dr. R. J. G.

Lewis. Seismographs and radio transceivers were loaned by the Australian Bureau of Mineral Resources. Both authors were supported by Commonwealth Postgraduate Research Awards.

## REFERENCES

- Asten, M. W., 1976, The use of microseisms in geophysical exploration: Ph.D. thesis, Macquarie University, North Ryde, N.S.W., Australia.
- 1977a, Measurement of phase velocities of microseisms with a small expanding seismic array in Proc. of Signal Processing for Arrays symposium, d'Assumpcao, H. A., Ed., Publication WRE-MISC-1, 80-92: Weapons Research Establishment, Salisbury, South Australia.
- 1977b, Theory and practice of geophone calibration in situ using a modified step method: Inst. of Elect. & Electron. Eng. Trans. of Geosci. Electronics, GE-15, 208-214.
- 1978a, Geological control on the three-component spectra of Rayleigh-wave microseisms: Bull. Seism. Soc. Am., 68, 1623-1636.
- 1978b, Phase velocities of mixed mode high-frequency microseisms (Abstract): Eos, 59, 1141.
- Bungum, H., and Capon, C., 1974, Coda pattern and multipath propagation of Rayleigh waves at NORSAR: Phys. Earth Planet. Inter., 9, 111-127.
- Capon, J., 1969, High resolution frequency-wavenumber analysis: Proc. Inst. Elect. and Electron Eng., 57, 1408-1418.
- 1970, Applications of detection and estimation theory to large array seismology: Proc. Inst. Elect. and Electron. Eng., 58, 760-770.
- 1973, Signal processing and frequency-wavenumber spectrum analysis for a large aperture seismic array, in Methods in computational physics, v. 13: Bolt, B. A., Ed., Academic Press Inc.
- Davies, D., 1973, Seismology with large arrays: Rep. Prog. Phys., 36, 1233-1283.
- d'Assumpcao, H. A., 1977, Some quadratic estimators for estimating directionality in Proc. of Signal Processing for Arrays Symposium, H. A. d'Assumpcao, ed., Publication WRE-MISC-1, 94-116: Weapons Research Establishment, Salisbury, South Australia.
- Dorman, J., 1959, Numerical solutions for Love wave dispersion on a half-space with double surface layer: Geophysics, 24, 12-29.
- Dorman, J., and Prentiss, D., 1960, Particle amplitude profiles for Rayleigh waves on a heterogeneous earth: J. Geophys. Res., 65, 3805-3816.
- Drake, L. A., 1972, Love and Rayleigh waves in non-horizontally layered media: Bull. Seism. Soc. Am., 62, 1241-1258.
- Eckart, C., 1953, The theory of noise in continuous media: J. Acoust. Soc. Amer., 25, 195-199.
- Ficken, F. A., 1967, Linear Transformations and Matrices: Prentice-Hall.
- Filson, J., 1975, Array seismology: Ann. Rev. of Earth and Planet. Sci., 3, 157-181.
- Goncz, J. H., and Hannan, E. J., 1975, New methods of estimating dispersion and stacks of surface waves: Bull. Seism. Soc. Amer., 65, 1519-1527.
- Hannan, E. J., 1975, Measuring the velocity of a signal in Perspectives in Probability and Statistics, Gani, J., Ed., Applied Probability Trust.
- Haubrich, R. A., and McCamy, 1969, Microseisms: coastal and pelagic sources: Rev. of Geophys., 7, 539-571.
- Henstridge, J., 1977, The measurement of velocity: Ph.D. thesis, Austral. Nat. Univ., Canberra, A.C.T., Australia.
- Koopmans, L. H., 1974, Spectral analysis of time series: Academic Press Inc.
- Kuo, J. T., and Thompson, G. A., 1963, Model studies on the effect of a sloping interface on Rayleigh waves: J. Geophys. Res., 68, 6187-6199.
- Lacoss, R. T., Kelly, E. J., and Toksöz, M. N., 1969, Estimation of seismic noise structure using arrays: Geophysics, 34, 21-38.
- Liaw, A. L., 1977, Microseisms in geothermal exploration: studies in Grass Valley, Nevada: Ph.D. dissertation, Lawrence Berkeley Laboratory, Univ. of Calif., Berkeley.
- Mayne, S. J., Nicholas, E., Bigg-Wither, A. L., Rasidi, J. S., and Raine, M. J., 1974, Geology of the Sydney Basin—A Review: Bull. 149, Canberra (Australia), Bureau of Mineral Resources, Geology and Geophysics.
- McEvilly, T. V., and Stauder, W., 1965, Effect of sedimentary thickness on short period Rayleigh-wave dispersion: Geophysics, 30, 198-203.
- Mooney, H. M., and Bolt, B. A., 1966, Dispersive characteristics of the first three Rayleigh modes for a single surface layer: Bull. Seism. Soc. Am., 56, 43-67.
- Pisarenko, V. F., 1972, On the estimation of spectra by means of non-linear functions of the covariance matrix: Geophys. J. Roy. Astr. Soc., 28, 511-531.
- Rao, C. R., 1973, Linear statistical inference and its applications, second edition: John Wiley, and Sons.
- Smart, E., 1971, Erroneous phase velocities from frequency-wavenumber spectral sections: Geophys. J. Roy. astr. Soc., 26, 247-253.
- Tatham, R. J., 1975, Surface wave dispersion applied to the detection of sedimentary basins: Geophysics, 40, 40-55.
- Toksöz, M. N., 1964, Microseisms and an attempted application to exploration: Geophysics, 24, 154-177.
- Toksöz, M. N., and Lacoss, R. T., 1968, Microseisms: mode structures and sources: Science, 159, 872-873.
- Widdow, B., Mantey, P. E., Griffiths, L. J., and Goode, B. B., Adaptive antenna systems: Proc. Inst. Elect. and Electron. Eng., 55, 2143-2159.
- Woods, J. W., and Lintz, P. L., 1973, Plane waves at small arrays: Geophysics, 38, 1023-1041.

## APPENDIX A

We may consider the case of only one signal by writing  $\zeta(\omega)$  as

$$\zeta(\omega) = N(\omega) + s(\omega)E(k_0)E(k_0)^*,$$

where

$N(\omega)$  is the component of the coherence matrix due to noise,

$s(\omega)$  is the spectrum of the signal,

and

$k_0$  is the wavenumber of the signal.

In what follows we shall drop the reference to  $\omega$  where it can be done without confusion.

With this model we have

$$\zeta^{-1} = N^{-1} - sN^{-1}E(k_0)E(k_0)^*N^{-1}/[1 + sE(k_0)^*N^{-1}E(k_0)],$$

(this can be shown by multiplying by  $\zeta$ ) and then the HR estimate is

$$\hat{P}(\omega, k) = \{E(k)^*N^{-1}E(k) - s[E(k)^*N^{-1}E(k_0)]^2/[1 + sE(k_0)^*N^{-1}E(k_0)]\}^{-1}.$$

The denominator in the last term can be expanded as a power series to give

$$\hat{P}(\omega, k) = [E(k)^*N^{-1}E(k)]^{-1} \sum_{r=0}^{\infty} \{s/[1 + sE(k_0)^*N^{-1}E(k_0)]\}^r \times |E(k)^*N^{-1}E(k_0)|^2/E(k)^*N^{-1}E(k)\}^{2r}. \quad (A-1)$$

The term  $|E(k)^*N^{-1}E(k_0)|^2/E(k)^*N^{-1}E(k)$  is similar to the adaptive filtering expressions of Widdow et al. (1967) and Henstridge (1977). In particular it achieves its maximum when  $E(k) = E(k_0)$  which implies  $k = k_0$  when spatial aliasing is not present. Hence the function given by the above summation would provide a good method of estimating  $k_0$ , but unfortunately it is then multiplied by  $[E(k)^*N^{-1}E(k)]^{-1}$  which will, in general, bias the position of the maximum of  $\hat{P}(\omega, k)$ . The biasing will only be absent if  $[E(k)^*N^{-1}E(k)]^{-1}$  is constant in a region about  $k_0$ . The only simple situation in which this occurs is when the noise at different stations is not correlated. Then  $N(\omega) = n(\omega)I$  where  $I$  is the identity matrix. Then

$$\hat{P}(\omega, k) = n/p \sum_{r=0}^{\infty} \left[ \frac{ps/n}{1 + ps/n} |E(k)^*E(k_0)|^2/p^2 \right]^{2r}, \quad (A-2)$$

and

$$\hat{P}(\omega, k) = n/p \left[ 1 - \frac{ps/n}{1 + ps/n} |E(k)^*E(k)|^2/p^2 \right]^{-1}. \quad (A-3)$$

This is clearly maximized when  $k = k_0$ , the maximum value being  $n/p + s$ .

The result should be compared with that obtained with the conventional beamforming estimate  $\hat{P}(\omega, k)$ .

If

$$\zeta(\omega) = nI + sE(k_0)E(k_0)^*, \quad (A-4)$$

then

$$\hat{P}(\omega, k) = np + s |E(k_0)^*E(k)|^2.$$

This will also achieve its maximum when  $k = k_0$  and the maximum will be  $np + sp^2$ . That is, in the case of one signal,  $\hat{P}$  and  $\hat{P}$  will give the same estimates of wavenumber and signal strength. The two spectra are monotonic functions of  $|E(k_0)^*E(k)|$  and as such will contain precisely the same information. The often mentioned high resolution of Capon's method does not apply in this case.  $\hat{P}(\omega, k)$  will have sharper peaks than  $\hat{P}(\omega, k)$ , particularly when the signal-to-noise ratio is high, because of the effects of the high powers in the summation in equation (A-2); but this does not imply greater accuracy.

## APPENDIX B

We may consider the case of several signals by modeling the spectral covariance matrix as

$$\zeta(\omega) = \varepsilon N(\omega) + U(\omega)S(\omega)U(\omega)^*,$$

where

$N(\omega)$  is the spectral density matrix of the noise as before,

$U(\omega)$  is a matrix whose columns are the phase vectors of the signals,

$S(\omega)$  is the spectral density matrix of the signals,

and

$\varepsilon > 0$  is a small number.

We do not assume that either  $N(\omega)$  or  $S(\omega)$  is a diagonal matrix. That is, the noise at different stations may be correlated, and different signals may be correlated. The only assumption is that the signals are not correlated with the noise. Using a result of Rao (1973, p. 33),

$$\zeta(\omega)^{-1} = \varepsilon^{-1} \{N^{-1} - N^{-1}U(U^*N^{-1}U)^{-1}U^*N^{-1}\}$$

$$+ \varepsilon N^{-1}U(U^*N^{-1}U)^{-1}[\varepsilon(U^*N^{-1}U)^{-1} + S]^{-1} \times (U^*N^{-1}U)^{-1}U^*N^{-1}.$$

We wish to consider the behavior of  $E(k)^*\zeta^{-1}(\omega)E(k)^*$ , as  $\varepsilon$  tends to zero, and we can do this by noting that  $E(k)$  can be represented as  $E(k) = Ua + b$  where  $a$  and  $b$  are vectors depending upon  $k$  and  $U^*N^{-1}b = 0$  (see, for example, Ficken, 1967, p. 299).

Then

$$E(k)^*\zeta^{-1}(\omega)E(k) = \varepsilon^{-1} \{b^*Nb + \varepsilon a^*[\varepsilon(U^*N^{-1}U)^{-1} + S]^{-1}a\}.$$

If  $k$  is the wavenumber of a signal, then  $E(k) = Ua$  where  $a$  will be a vector with a 1 in the appropriate position and zeros elsewhere. Then since  $b = 0$

$$\hat{P}(\omega, k) = \{a^*[\varepsilon(U^*N^{-1}U)^{-1} + S]^{-1}a\}^{-1},$$

and as  $\varepsilon$  tends to zero, this goes to  $(a^*S^{-1}a)^{-1}$  which will be nonzero since  $S$  is positive definite. However, if  $k$  does not correspond to a signal, then  $b$  will not be zero, and the term  $\varepsilon(b^*Nb)^{-1}$  will dominate as  $\varepsilon$  tends to zero so that  $\hat{P}(\omega, k)$  will tend to zero. Thus in the limit,  $\hat{P}(\omega, k)$  will be zero except when  $k$  corresponds to the wavenumber of a signal present.